

Impact of

on the

~~How much does the snow surface influence ice crystal concentration measurements at mountain-top stations~~

or

~~Does it make sense to measure ice crystal number concentration at mountain-top stations?~~

Alexander Beck¹, Jan Henneberger¹, and Ulrike Lohmann¹

¹Institute for Atmospheric and Climate Sciences, ETH Zurich, Zurich, Switzerland

Key Points:

- In-situ measurements of microphysical cloud properties with a holographic Imager
- Influence of in-situ cloud observations at mountain top stations by ground based ice enhancement processes
-

13 Abstract

14 In-situ cloud observations at mountain-top research station regularly measure ice crystal
 15 number concentrations (ICNCs) orders of magnitudes higher than expected from mea-
 16 surements or simulations of ice nuclei particle concentrations. Several studies suggest ~~that~~
 17 mountain-top in-situ measurements are influenced by surface-based ice-enhancement pro-
 18 cess, e.g. blowing snow, hoar frost or riming on snow covered trees, rocks and the remain-
 19 ing snow surface. A strong influence of in-situ observations on mountain-top stations by
 20 surface-based ice-enhancement processes may limit relevance of such measurements and
 21 could have an impact on orographic clouds. ~~the~~

22 This study assesses the influence of surface-based ice-enhancement processes on
 23 in-situ cloud observations at the Sonnblick Observatory in the Hohen Tauern Region,
 24 Austria. Vertical profiles of ICNCs above a snow covered surface were observed up to
 25 a height of 10 m. A decrease of the ICNC by at least a factor of two is observed, if the
 26 maximum ICNC is larger than 1001^{-1} . This decrease ~~can be~~ extended up to one order of mag-
 27 nitude during in cloud conditions and reached its maximum of ~~more than~~ two orders of
 28 magnitudes when the station was not in cloud. On one day a relative decrease of the ICNC
 29 of regular and irregular ice crystals was observed with height, which can't be explained by
 30 surface-based ice-crystal enhancement processes. A mechanism is proposed that possibly
 31 enhances the ICNC close to the surface when cloud particles sediment and are captured
 32 in a turbulent layer above the surface. These observations strongly suggest that mountain-
 33 top in-situ measurements poorly represent the true properties of the cloud in contact with
 34 the surface. They are influenced not only by surface-based ice-enhancement processes, but
 35 possibly also by ICNC enhancement due to turbulent layers above the surface.

36 1 Introduction

37 The microphysical properties (e.g. phase composition, cloud particle number con-
 38 centrations) and cloud processes are key parameters for the clouds lifetime, the cloud ex-
 39 tent, as well as the intensity of precipitation they produce [Rotunno and Houze, 2007]. For
 40 example, the phase composition influence the radiative properties of midlevel clouds in
 41 the temperature range between 0 to -35 °C. A pure ice cloud in this temperature regime
 42 reflects 17 W m⁻² more radiation than a pure liquid cloud [Lohmann, 2002]. A well rep-
 43 resentation of orographic mixed-phase clouds is therefore crucial for accurate weather pre-
 44 dictions in alpine terrain and improved climate models.

45 In-situ measurements are important to improve our understanding of microphysical
 46 properties and fundamental processes of orographic mixed-phase clouds [Baumgardner
 47 et al., 2011] and are frequently conducted at mountain-top research stations. Despite an
 48 improved understanding on the origin of ice crystals from nucleation (citation!!!!) as well
 49 as from secondary ice-multiplication processes [Field et al., 2017], the source of most of
 50 the ice crystals observed at mountain-top stations and their impact on the development of
 51 the cloud remains an enigma (citation!!!!). ~~Lohmann et al. 2016~~

52 In-situ observations with aircraft usually observe ~~an~~ ICNC on the order of $1-101^{-1}$
 53 [Gultepe et al., 2001], whereas at mountain-top research stations (e.g. Elk Mountain, USA
 54 or Jungfraujoch, Switzerland) or near the snow surface in the Arctic ICNCs of several
 55 hundreds to thousands per liter are frequently reported [Rogers and Vali, 1987; Lachlan-
 56 Cope et al., 2001; Lloyd et al., 2015]. Secondary ice multiplication processes like frag-
 57 mentation [Rangno and Hobbs, 2001] or the Hallett-Mossop process [Hallet and Mossop,
 58 1974] are usually ruled out as the source for the observed ice crystals due to the lack of
 59 large ice crystals, respectively large cloud droplets or the wrong temperature range. In-
 60 stead surface-based ice-enhancement processes are proposed to produce such enormous
 61 ICNCs. Rogers and Vali [1987] suggested two possible processes as a source for the ob-
 62 served ICNC: riming on trees, rocks and the snow surface or the lifting of snow particles
 63 from the surface, i.e. blowing snow. In addition, Lloyd et al. [2015] suggested hoar frost

as a wind independent, surface-based ice-enhancement process to cause ICNCs larger than $100\text{ }\mu\text{m}^{-1}$ for which they did not observe a wind dependency as expected for blowing snow. Although different studies are ~~strife~~ about the mechanisms to explain the measured high ICNCs, they agree on a strong influence by surface-based processes.

While the influence of mountain-top measurements by surface-based processes is widely accepted, the impact of re-suspended ice crystals on the development of super-cooled orographic clouds, e.g. a more rapid glaciation and enhanced precipitation, has not been studied extensively [Geerts et al., 2015]. If the proposed surface-based ice-enhancement processes have the potential to impact the development of a cloud depends primarily on the penetration depth of the resuspended particle into a cloud, i.e. the maximum height above the surface to which the particles get lifted.

The height dependency of blowing snow has been studied in the context of snow redistribution ("snow drift") and reduced visibility due to the re-suspended ice crystals by observing ice crystals up to several meters above the snow surface [Schmidt, 1982; Nishimura and Nemoto, 2005]. It has been reported that blowing snow occurs above a wind speed threshold that varies between 4 m s^{-1} and 13 m s^{-1} [Brown, 1988; Li and Pomeroy, 1997; Mahesh et al., 2003; Dery and Yau, 1999]. Besides the wind speed, the concentration of blowing snow depends on the snowpack properties () and on the atmospheric conditions (current temperature, humidity) [Vionnet et al., 2013]. Nishimura and Nemoto [2005] observed the ICNCs up to a height of 9.6 m and found that the ICNCs usually decrease to as low as 1-10 particles per liter. During a precipitation event, the relative importance of the small ice crystals below $< 100\text{ }\mu\text{m}$ decreases from nearly 100 % at 1.1 m to below 20 % at 9.6 m. The rapid decrease of ICNCs with height observed by these studies may limit the impact of blowing snow on orographic clouds. However, most of these studies were conducted in dry air conditions where ice crystals undergo rapid sublimation [Yang and Yau, 2008], which may limit the applicability of these results.

Lloyd et al. [2015] suggested that vapor grown ice crystals on the crystalline surface of the snow cover, i.e. hoar frost, may be detached by mechanical fracturing due to turbulence independent of wind speed. To our knowledge only one modelling study exists, which assesses the impact of hoar frost on the development of a cloud. Farrington et al. [2015] implemented a flux of surface hoar crystals in the WRF (Weather Research and Forecasting) model based on a frost flower aerosol flux to simulate ICNCs measured at the Jungfraujoch by Lloyd et al. [2015]. They concluded that the surface-based ice crystals have a limiting impact on orographic clouds because the ice crystals are not advected high into the atmosphere. However, more measurements of ice crystal fluxes from the snow-covered surface are necessary to simulate the impact of surface-based ice crystal enhancement processes on the development of orographic clouds [Farrington et al., 2015].

In contrast to these findings, several remote sensing (i.e. satellite, lidar and radar) studies measured ice crystals advected as high as 1 km above the surface, which suggests an impact of surface-originated ice crystals on clouds. Satellite observations of blowing snow from MODIS and CALIOP over Antarctica [Palm et al., 2011] observed layer thickness up to 1 km with an average thickness of 120 m for all observed blowing snow events. Similar observations from lidar measurements exist from the South Pole with an observed layer thickness of ice crystals of usually less than 400 m, in some rare cases when a subvisual layer exceeded a height of 1 km [Mahesh et al., 2003]. However, a possible suspension of clear-sky precipitation could not be ruled out as a source of the observed ice crystal layers. Observations of layers of ice crystals from radar measurements on an aircraft in the vicinity of the Medicine Bow Mountains [Vali et al., 2012] observed ground-layer snow clouds which were most of the time not visually detectable but produced a radar signal. Resuspended ice crystals from the surface or riming of cloud droplets at the surface can be the origin of the ice crystals in such ground-layer snow clouds. Geerts et al. [2015] presented evidence for ice crystals becoming lofted up to 250 m in the atmosphere by boundary layer separation behind terrain crests and by hy-

117 draulic jumps. Also evidence that ice crystals from the surface may lead to the glaciation
 118 of supercooled orographic clouds and enhanced precipitation were found. However, Geerts
 119 ~~et al.~~ [2015] also mention the limitation of radar and lidar measurement to separate the
 120 small ice crystals produced by surface processes from the larger falling snow particles
 121 and more abundant cloud droplets. They even concluded, that "to explore BIP (blowing
 122 snow ice particle) lofting into orographic clouds, ice particle imaging devices need to be
 123 installed on a tall tower, or on a very steep mountain like the Jungfraujoch".

124 In this study we assess the influence of surface-based ice-enhancement processes
 125 on in-situ cloud observations at mountain-top stations and the potential impact on orographic
 126 mixed-phase clouds. Vertical profiles of the ICNC up to a height of 10 m above
 127 the surface were observed for the first time on a high-altitude mountain station with the
 128 holographic imager HOLIMO [Beck *et al.*, 2017]. HOLIMO is capable of imaging ice
 129 crystals larger than $25 \mu\text{m}$ and the shape of these ice crystals can be analyzed.

130 2 Field Measurements at the Sonnblick Observatory

131 2.1 Site description

132 This field campaign was conducted at the Sonnblick Observatory (SBO) situated at
 133 the summit of Mt. Sonnblick at 3106 masl ($12^{\circ}57' \text{E}$, $47^{\circ}3' \text{N}$) in the Hohen Tauern National
 134 Park in the Austrian Alps. The SBO is a meteorological observatory operated all
 135 year by the ZAMG (Central Institute for Meteorology and Geodynamics). On the ~~East~~ and
 136 ~~South~~ the SBO is surrounded by large glacier fields with a moderate slope, whereas on the
 137 ~~Northeast~~ a steep wall of approximately 800 m descends to the valley (Fig. 1, right). Part
 138 of the SBO is a 15 m high tower used for meteorological measurements by the ZAMG.
 139 The data presented in this paper was collected during a field campaign in February 2017.

140 2.2 Instrumentation

141 The properties of hydrometeors were observed with the holographic ~~Imager~~ HOLIMO,
 142 which is part of the HoloGondel platform [Beck *et al.*, 2017]. The holographic ~~Imager~~ was
 143 mounted on an elevator that was attached to the meteorological tower of the SBO (Fig. 2)
 144 to obtain vertical profiles of the hydrometeor properties up to a height of 10 m above the
 145 surface where the platform was repeatedly positioned at five different heights as indicated
 146 in Figure 2. The holographic imager HOLIMO had a distance of approximately 1.5 m
 147 from the tower on the east-northeast side of the tower (Fig. 1, right).

148 The holographic imager HOLIMO yields single particle informations, e.g. size, and
 149 shadowgraphs from all cloud particles in a three-dimensional volume on a single image,
 150 a so-called hologram. Per hologram, a sample volume of 16 cm^3 with a length of 6 cm
 151 along the optical axis is examined. Concentrations and particle size distributions are cal-
 152 culated over 50 holograms corresponding to a volume of 800 cm^3 . The open source soft-
 153 ware HoloSuite [Fugal, 2017] is used to reconstruct the in-focus images of the particles.
 154 Particles smaller than $25 \mu\text{m}$ are classified as liquid droplets, whereas particles larger
 155 than $25 \mu\text{m}$ are separated in liquid droplets and ice crystals based on the shape of their
 156 2D image. Similar to a study by Schlenzeck and Fugal [2017] the ice crystals were further
 157 visually classified into three different groups: regular, irregular and aggregates. Because
 158 the visual classification of several thousands of ice crystals is time consuming this sub-
 159 classification of ice crystals was done only for the profiles on February 17th.

160 *by point analysis* A single vertical profile was observed within a time interval of 10-12 min. There-
 161 fore, the holographic imager HOLIMO was positioned at an individual height for 2 min and
 162 holograms were recorded at 4 fps. This results in 81 of sampled air.

163 Meteorological data are available from the measurements by the ZAMG. The ZAMG
 164 measures one minute averages of temperature, relative humidity and horizontal wind speed

165 and direction at the top of the meteorological tower. Snow cover depth is daily manually
 166 observed by the operators of the SBO. Based on these measurements the change of the
 167 snow cover is calculated. However, this calculation includes all the changes in the snow
 168 cover depth, e.g. snow drift, sublimation, melting and fresh snow. Daily measurements of
 169 the total precipitation are available on the ~~North~~ and ~~South~~ side of the SBO. A ceilometer
 170 located in the valley ~~on the~~ North of the SBO measured the cloud base and cloud depth.
 171

172 In addition, a 3D sonic anemometer was mounted at the top of the meteorological
 173 tower. However, data is only available occasionally, because most of the time the heating
 174 of the anemometer was not sufficient ~~enough~~ to prevent the build up of rime on the mea-
 surement arms.

175 3 Results

176 The data presented were observed on 4 February and 17 February 2017. Figure 3
 177 and 4 show an overview on the meteorological conditions on both days. The main differ-
 178 ence is the wind direction, which was ~~South West~~ on 4 February and ~~North~~ on 17 Febru-
 179 ary.

180 Case study on 3.1 4 February 2017

181 On 4 February a low pressure system moved eastwards from the Atlantic Ocean over
 182 northern France to western Germany, where it slowly dissipated. Influenced by this low
 183 pressure system the wind at the SBO predominantly came from ~~West-Southwest~~ and wind
 184 speeds between 10 and 25 m s⁻¹ (Fig. 3). In the late afternoon, around 1900 UTC, when
 185 the low pressure system dissipated over western Germany, the wind direction changed to
 186 ~~North~~ and wind speeds decreased to a minimum of 5 m s⁻¹. After 1900 UTC wind speed
 187 increased again to up to 15 m s⁻¹. Starting from 0800 UTC the SBO was in cloud except
 188 for a short time interval between 1910 and 2020 UTC. Because no data is available from
 189 the 3D sonic anemometer, only one minute averages are available from the ZAMG mea-
 190 surements.

191 The temperature didn't change much during the day and stayed between -10 and -
 192 9 °C until 1900 UTC when the wind direction changed to ~~North~~ and the temperature de-
 193 creased to -11 °C at 22 UTC.

194 Between 0830 and 2200 UTC, a total of 24 vertical profiles were obtained. Most
 195 of the profiles were obtained when the station was in cloud except for four profiles be-
 196 tween 1910 and 2020 UTC (blue shaded in Fig. 3). The ICNC reaches a maximum at
 197 2.5 m above the surface (Fig. 5). Compared to this maximum, the mean ICNC at a height
 198 of 10 m decreased by a factor of two and the median ICNC even by a factor of four. These
 199 strong decrease of ICNC with height suggest that the majority of the ice crystals near the
 200 ground originate from the snow surface.

201 The whole measurement time period during the 4 February was divided in four pe-
 202 riods representing different conditions (Fig. 6). Between 1910 and 2010 UTC (Fig. 6
 203 third row), when the SBO was not in cloud, the ICNC have their maximum at a height
 204 of 2.5 m. The maximum ICNC at this height reaches up to 600 l⁻¹. For three of the pro-
 205 files, the ICNC decrease by more than a factor of 5 from over 100 l⁻¹ at 2.5 m to less than
 206 20 l⁻¹ at 10 m. The mean ICNC decreases from around 100 l⁻¹ at 2.5 m to 10 l⁻¹ at 10 m
 207 (Fig. 6, right panel in the third row). The large extent of the shaded area at 2.5 m rep-
 208 resents the high variability of the ICNC even when the data is averaged over 800 cm³.
 209 Because the SBO was not in cloud during this time period, these measurements strongly
 210 suggest that up to several hundreds of ice crystals per liter originated from surface-based
 211 processes at a height of 2.5 m and at a wind speed of less than 10 m s⁻¹.

~~days must be 50~~

212 Between 2030 and 2200 UTC (Fig. 6 first row), when the SBO was in cloud again,
 213 the vertical profiles of the ICNC show a similar tendency as in the cloud free period. The
 214 maximum of the ICNC was observed at a height of 4.1 m and the ICNC decreases
 215 consistently for all four profiles with height above the ~~observed maximum~~. The mean of the
 216 ICNC decreased by a factor of 9 from its maximum at 4.1 m to its minimum at 10 m. This
 217 decrease is in the same order of magnitude as in the cloud free case discussed above. As
 218 assuming that the observed ICNC at 10 m is representative for the cloud without surface
 219 influence, the surface-based processes contribute with several hundreds of ice crystals per
 220 liter to the measurements at 2.5, 4.1 and 6.0 m. This surface-based contribution is in the
 221 same order of magnitude as the total measured ICNCs in the cloud free period observed
 222 between 1910 and 2020 UTC. In contrast to the cloud free period, the surface influence
~~now~~
 223 extends to a height of 6.0 m, which can be explained by the increased wind speed of up to
 224 15 m s⁻¹.

225 The highest ICNCs were observed in the time period between 1200 and 1500 UTC
 226 (Fig. 6 second row) when also the wind speed reached its maximum of 25 m s⁻¹. The box-
 227 plot shows a maximum ICNC at 2.5 m in the range of 500 to 900 l⁻¹ and a decrease by a
 228 factor of 2 within 7.5 m. This decrease is much lower than observed in the previous time
 229 interval and is most likely due to the high wind speeds. Between different profiles the
 230 ICNC changed by a factor of ??? however, the trend of a decreasing ICNC with height
 231 was observed consistently for all profiles.

232 In the morning between 0830 and 1100 UTC the observed ICNCs (Fig. 6 first row)
 233 are much lower than between 1200 and 1500 UTC, although wind speed was as high as
 234 20 m s⁻¹. A possible reason is that the last snow fall was observed ??? days before the
 235 measurement. During these time, the loose ice crystal at the surface where blown away
 236 and the snowpack was solidified by temporal melting and re-freezing the snowpack [Kann
 237 man das so schreiben?]. Consequently, higher wind speeds are necessary to resuspend ice
 238 crystals from the snowpack.

239 The correlation between wind speed and ICNC ~~on~~ a 1 min time scale is shown in
 240 Figure 7. The maximum wind speed is used rather the average wind speed, because it is
 241 expected that the gusts, i.e. the highest wind speed in an time interval are most relevant
 242 for resuspending ice crystals from the surface. For the time interval between 0830 an 1500
 243 UTC when the wind direction was west-southwest no correlation is observed with wind
 244 speeds higher than 14 m s⁻¹ (Fig 7, top). For the time interval between 1910 and 2230
 245 UTC, when the wind direction was north, a much more pronounced dependency of the
 246 ICNC on wind speed is observed for wind speeds lower than 14 m s⁻¹ (Fig 7, bottom).
 247 ICNCs reached a saturation for wind speed larger than 14 m s⁻¹.

any explanation for this?

248 3.2 17 February 2017

249 On 17 February a cold front over northern Europe was moving southwards causing
 250 mainly northerly flow across the Alps and at the SBO (Fig. 4). Wind speeds observed at
 251 the SBO in the time interval between 1800 and 2000 UTC were between 5 and 10 m s⁻¹.
 252 In the same time interval temperature decreased by 1 K from -12.5 to -13.5 °C. The SBO
 253 was in cloud starting from 1300 UTC with varying visibility between several meters up to
 254 several hundreds of meters. Some snow fall was observed in the afternoon between 1300
 255 and 1500 UTC.

256 For this day, wind data of the 3D Sonic Anemometer are available, which allow a
 257 more detailed analysis of the correlation between the observed ICNC and wind speed. Un-
 258 fortunately, only four vertical profiles were obtained due to hardware problems with the
 259 computer. The first profile was measured in the morning at 1200 UTC when the SBO was
 260 not in cloud and no ice crystals were observed. Three more profiles were observed in the
 261 late afternoon starting from 1800 UTC. For these profiles the ice crystals have been classi-
 262 fied by hand and subclassified in the three categories: regular, irregular and aggregates.

~~entire wind from N
order wind direction
was IV~~

The three profiles observed in the late afternoon of 17 February showed ICNCs of several hundreds in the lowest height intervals with a maximum between 4.1 and 6.0 m (Fig. 8). The minimum ICNC was consistently observed for all profiles at 10 m and was always below 150 l^{-1} . The decrease of the ICNC with height varies between a factor of 2 and 4. In general the observed profiles on this day are similar to the ones observed on 4 February between 2030 and 2200 UTC when similar meteorological conditions were present. Wind direction was mainly from North to Northeast and wind speed varied between 5 and 10 m s^{-1} in both measurement intervals. Only temperature was slightly lower on 17 February.

In contrast to the data of 4 February, no correlation between ICNCs and the horizontal wind speed is observed (Fig. 9). This holds true for the one minute averages and maximum wind speeds observed by the SBO as well as the one second averages observed with the 3D sonic anemometer. However, the ICNC increased with the vertical wind speed. *because more crystals were nucleated (oder warm)*

All the ice crystals observed on 17 February were classified by hand into aggregates, irregular and regular ice crystals (Fig. 10). ICNCs are dominated by irregular ice crystals, which is in good agreement with various other observations (citations). However, it is surprising that the relative importance of the irregular ice crystals stays constant with height or even increases (Fig. 10 right panels). Surface-based ice-crystal enhancement processes are expected to produce irregular ice crystals. With increasing height this influence is expected to decrease and regular ice crystals are expected to become more important. However, from this data a proportional decrease of the absolute number of regular and irregular ice crystals is observed and is in contradiction to the expectations from surface-based ice-crystal enhancement processes. A further discussion of these results will follow in section 4.1. The wind dependency of the ICNC of irregular and regular ice crystals is comparable, and both increase by a factor of 2 when the vertical wind speed increased from $0\text{-}2 \text{ m s}^{-1}$ to $4\text{-}6 \text{ m s}^{-1}$ (Fig. 11). Whereas the shape of the size distribution of the irregular ice crystals does not vary much with height, larger regular ice crystals are stronger reduced than smaller regular ice crystals (Fig. 12).

4 Discussion

4.1 Comparison with the properties of blowing snow observed in the Arctic

To better understand if the observed ice crystals are re-suspended from the surface, the results of 17 February are compared to the properties of blowing snow observed in the Arctic ([Nishimura and Nemoto, 2005]) and further discussed.

It is expected that the majority of the ice crystal re-suspended from the surface have irregular habits, whereas regular ice crystals originated in cloud. Furthermore, for the re-suspended ice crystals a decrease of the ICNC is expected with height, with a stronger decrease of the larger ice crystals. This results in a shift of the size distribution to smaller sizes or a decrease of the mean particle diameter with height, as it was also observed by Nishimura and Nemoto [2005]. However, the strongest decrease of the size of the ice crystals was observed below 1 m above the snow surface, whereas the size of the ice crystals stayed fairly constant in the range of $70\text{-}100 \mu\text{m}$ in the height between 1 and 9.6 m. It is important to notice that Nishimura and Nemoto [2005] measured the properties of blowing snow above a flat surface in dry air. Sublimation of ice crystals in such an environment additionally reduces the ice crystals diameter. *above ground*

For a better comparison a two-parameter gamma probability density function (gamma-pdf) [Budd, 2013; Schmidt, 1982]

$$f(d) = \frac{d^{\alpha-1}}{\beta^\alpha \Gamma(\alpha)} \exp\left(-\frac{\beta}{d}\right) \quad (1)$$

with the particle diameter d , the shape parameter α and the scale parameter β is fitted to the results of 17 February for both regular and irregular ice crystals (Fig. 13). The resulting shape parameter α and the mean diameter, represented by the product of the shape and scale parameter of the gamma-pdf, are plotted in Figure 14.

The mean diameter for both the irregular and regular ice crystals is in the range of the properties of blowing snow, with a decrease from 120 to 70 μm for regular ice crystals and a rather constant mean diameter of 100 μm for irregular ice crystals (Figure 14 left). Nishimura and Nemoto [2005] observed a strong increase of the shape factor from 3 to 10 between 1 and 9.6 m. Whereas the shape parameter obtained for the regular ice crystals increases with height, it stays constant for the irregular ice crystals. Most important a decrease of the ICNC for both the irregular and regular ice crystals by a factor of 2 is observed within a height interval of 7.5 m (Fig. 8). All these findings suggest that the majority of the irregular as well as the regular ice crystals are re-suspended from the snow surface. However, this contradicts our assumptions that the majority of the regular ice crystals originate in cloud and only irregular ice crystals are re-suspended from the surface, as it is observed between 1910 and 2000 UTC on 4 February, for what an inspection of the ice crystal habits by eye showed almost exclusively irregular crystals and therefore is considered a blowing snow event. As a consequence, either our assumptions are wrong and also regular ice crystals contribute to the ICNC of re-suspended particles or a different mechanism has to be responsible for the enriched ICNC close to the snow surface (Fig. 10).

During the measurements on 17 February the SOB was in cloud. Ice crystals of irregular and regular habits originated in cloud sediment and may be kept floating near the surface due to turbulence that is also responsible for the re-suspension of ice crystals from the surface. However, in this case the sedimenting particles may have never reached the surface and maintained their habit. Such an effect may also enrich ICNCs observed close to the surface, but in this case a snow covered surface is not necessary and the wind threshold is much lower than for surface-based ice crystal enhancement processes, because ice crystals do not have to be detached from the surface. This can explain the observation of high ICNCs on 17 February also the wind speed was in most cases close to the lower threshold wind speed observed for blowing snow, which is 4 m s^{-1} [Bromwich, 1988; Li and Pomeroy, 1997; Mahesh et al., 2003; Dery and Yau, 1999]. The result of such a mechanism is a rather constant ICNC above the surface and a similar decrease of the ICNC of regular and regular ice crystals with height, as it was observed on 17 February.

Although it is proposed that ICNC is dominated by a mechanism just described, blowing snow still contributes to the ICNC at certain time intervals. During one profile (Fig. 10, top row) the ICNC decreases for irregular and regular ice crystals with exception for the irregular ice crystals at a height of 6 m. Whereas the vertical wind speed during this profile was similar for all heights at 4 m s^{-1} , it reached a maximum of 5.5 m s^{-1} when the elevator was positioned at 6 m, This corresponds with the increased ICNC of the irregular ice crystals whereas the concentration of regular ice crystals was not affected. This suggests that ice crystals re-suspended from the surface have reached the height of 6 m during higher wind speeds and had dominantly irregular habits.

The difference in the height dependence of the size distribution of regular and irregular ice crystals remains unexplained. Whereas the irregular ice crystals show a constant decrease of the ICNC over all sizes, the size distribution for regular ice crystals is shifted to smaller sizes with increasing height. A possible reason for the decrease of the mean diameter of the regular ice crystals is that the particles in the turbulent layer above the surface grow due to vapor diffusion before they final fall out. Therefore regular ice crystals

aber das würde die irregularen Eiskristalle gleichermaßen betreffen

smaller (?)

closer to the surface are larger than the regular ice crystals in cloud. The shift of the size distribution is caused by smaller ice crystals that just sediment and have not been captured in the turbulent layer. These ice crystals become more important with height and start to dominate the size distribution. *wie? Sie kleiner*

364 4.2 Wind dependency of the observed ICNCs

365 The observations on 4 February and 17 February show a different correlation of the
 366 ICNC with wind speed. The ICNCs observed on 4 February show a dependency only for
 367 horizontal wind speed below 14 m s^{-1} (Fig. 9), whereas for horizontal wind speeds larger
 368 than 14 m s^{-1} this correlation is probably not observed due to a saturation of blowing
 369 snow. On 17 February a correlation is only observed with vertical wind speed available
 370 from the 3D sonic anemometer (Fig. 9). Possibly, the vertical wind speed is a better ap-
 371 proximation for the turbulence responsible for the re-suspension of ice crystals from the
 372 surface as it was already suggested by Hammer *et al.* [2014]. In addition vertical wind
 373 speeds may play an important role especially at research stations like the SBO and the
 374 High Altitude Research Station Jungfraujoch, Switzerland, because ice crystals may be
 375 transported from below the research station to the measurement point. For example [Lloyd
 376 *et al.*, 2015] observed a dependency on horizontal wind speeds only for ICNCs smaller
 377 than $100 \mu\text{m}$, whereas larger ICNCs didn't show a dependency on horizontal wind speed.
 378 Blowing snow, respectively hoar frost were proposed as the underlying mechanisms for
 379 these observations. We suggest that the larger ice crystals observed by Lloyd *et al.* [2015]
 380 had been transported for a longer time and grown to larger sizes. In this case the vertical
 381 wind speed could be more relevant, because the particles may have been transported from
 382 the research station by vertical winds. *could include on suitable INP and/or or*

383 It has to be mentioned that various difficulties exist when it comes to observing the
 384 correlation between wind speed and ICNCs. Firstly, ICNCs are usually compared to a
 385 simultaneously measured wind speed. However, the observed ice crystals have been re-
 386 suspended some time before the measurement and transported in the air for some time. In
 387 this case the simultaneously observed wind speed is not necessarily the driving force of
 388 the process of particle lifting, because ice crystals that were re-suspended from the surface
 389 by strong turbulence can be transported higher in the atmosphere by much smaller wind
 390 speeds (blowing snow paper). Secondly, wind and ICNC measurements may be performed
 391 at two different locations. Especially at mountain-top research station with its many struc-
 392 tures, local turbulence responsible for the re-suspension of the observed ice crystals may
 393 be not well represented by such a wind measurement. This is also true for this study,
 394 where the wind measurement was located on a 15 m high meteorological tower. Thirdly,
 395 the ICNC does not only depend on wind speed, but also on age of the snow cover and
 396 atmospheric conditions and a possible correlation may be suppressed in a data set with dif-
 397 ferent snowpack and atmospheric conditions. Between 1900 and 2030 UTC on 4 February
 398 a decrease of the ICNC was observed with time at a height of 2.5 m, possibly because the
 399 very loose ice crystals on top of the snow cover were blown away. *Watum dient Sedimen-
 400 tation der Kristalle?*

400 Another crucial point for correlating observed ICNCs to wind speed is the average time
 401 of the data. If the averaging time is small, e.g. 1 m it is assumed that the observed
 402 ice crystals were re-suspended close to the measurement point and immediately trans-
 403 ported. If the average time is very large, the effect of blowing snow may be averaged out.
 404 In this study we chose an average time of 10-15 s. This assumes that the particles were
 405 re-suspended ~~at most~~ ~~up to~~ *maximal* 50-100 m apart from the measurement point and it is believed that
 406 also peaks of large concentration are not yet averaged out.

407 **4.3 Influence of ICNC measurements by a snow surface at mountain-top stations**
 408 **and its impact on clouds**

409 The results obtained in this study suggest a strong enhancement of the ICNC mea-
 410 sured close to the snow surface at mountain-top research stations. On 4 February a blow-
 411 ing snow event was observed when the SBO was not in cloud and the ICNC was en-
 412 hanced by a factor of 100 at a height of 2.5 m when compared to upper levels of the el-
 413 evator (Fig. 6, second row). When the SBO was in cloud an enhancement by a factor of
 414 2-10 was observed in the same height interval. On 17 February a similar decrease of the
 415 ICNC was observed for irregular and regular ice crystals. This is ~~in~~ contrast to the expecta-
 416 tions for blowing snow and a different mechanism is proposed, which enhances the ICNC
 417 close to the surface when sedimenting ice crystals ~~are~~ captured in turbulence. The observed
 418 ICNC close to the surface is also at least 2 times larger than at a height of 10 m. There-
 419 fore, we propose that measurements of the ICNC close to the surface ~~can't~~ represent real
 420 cloud properties.

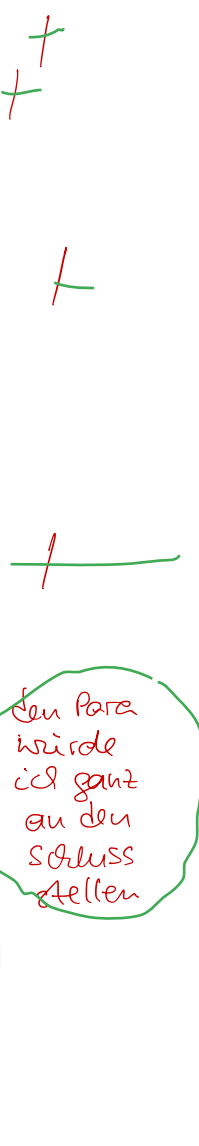
421 An estimation of the influence of cloud properties by re-suspended ice crystals is
 422 difficult, because of the limited vertical extent ~~of~~ the profiles obtained in this study. For
 423 most of the profiles the ICNC still shows a decreasing tendency at a height of 8-10 m and
 424 a final statement of the in-cloud ICNC is not possible. Only for the profiles after 1900
 425 UTC a constant ICNC is observed for the upper levels of the elevator (Fig. 6, two bot-
 426 tom rows). From the observation between 2030 and 2200 UTC, when the SOB was in
 427 cloud, the ~~in~~ cloud ICNC can be estimated, when the observed ICNC during the blowing
 428 snow event between 1900 and 2000 UTC is subtracted for the upper levels of the eleva-
 429 tor. This results in a ICNC of several tens per liter. Between 1200 and 1500 UTC (Fig.
 430 6, second row) the wind speed was much higher and the influence of blowing snow pos-
 431 sibly extends ~~to~~ much higher up in the atmosphere. Because the number of ice nucleating
 432 particles in clouds is on the order of ~~1-10~~¹⁻¹⁰, already ice crystals of the same concentra-
 433 tion re-suspended from the surface and lifted high up into the cloud can have a significant
 434 impact on the clouds properties, e.g. extent and lifetime.

435 To better understand the mechanisms that are responsible for an enhanced ICNC
 436 close to the surface and to further investigate the mechanisms proposed in this study we
 437 suggest a more thorough field campaign with additional 3D sonic anemometer at the
 438 surface to capture turbulence that may be responsible for the re-suspension of ice crys-
 439 tals, a second 3D sonic anemometer on the elevator and a third 3D anemometer on the top
 440 of the tower. This may help to better understand the wind dependence ~~of~~ of the ICNC and
 441 help to find the origin of the observed ice crystals. At ~~the best at least~~ three cloud imaging
 442 probes are part of such a campaign and installed parallel to the 3D sonic anemometer.
 443 In addition, to get a better estimate of the impact of re-suspended particle on cloud por-
 444 ties, especially for high wind speeds, the vertical profiles have to be extended to larger
 445 heights above the surface. Such a field campaign could be conducted using a tethered bal-
 446 loon system equipped with cloud imaging probes, which can be lifted several hundreds of
 447 meters into the atmosphere.

448 **5 Conclusion & outlook**

449 This study assess the influence of mountain-top in-situ measurements by surface-
 450 based ice-crystal sources and possible implications on atmospheric relevance of such mea-
 451 surements. An elevator was attached to the meteorological tower of the SBO, Austria and
 452 vertical profiles of the ICNC were observed with the holographic imager HOLIMO on two
 453 days in February 2017. The main findings are:

- 454 • ICNCs decrease with height. ICNCs near the ground are at least a factor of two
 455 ~~larger~~ smaller than at a height of 10 m (if the ICNC near the ground is larger than 100 l^{-1}).
 456 The increase in ICNCs near the ground can be up to an order of magnitude during



457 cloud events and even two magnitudes during cloud free periods. Therefore, in-situ
 458 measurements of the ICNC at mountain-top research stations close to the surface
 459 overestimate the ICNC.

- 460 • On 4 February ICNCs show a dependency ~~on~~² on wind speed up to 14 ms^{-1} . For higher
 461 wind speeds the ICNCs due to surface-based ice-crystal enhancement processes are
 462 possibly saturated.
- 463 • On 17 February a similar decrease of the concentration of irregular and regular ice
 464 crystals is observed with height, which can not be explained by surface-based ice
 465 crystal enhancement processes. Sedimenting ice crystals ~~not~~^{are} possibly capture in a
 466 turbulent layer close to the surface and enhances ICNCs similar to blowing snow.
 467 However, because the ice crystals actually never had contact with the surface, their
 468 habits are obtained ~~preserved~~^{ICNC}.
- 469 • The strong influence of surface-based ice-crystals sources on the measurements
 470 on mountain-top stations limits the atmospheric relevance of such measurements.
 471 However, the data set obtained is ~~to~~^{too} small to make a clear statement under which
 472 conditions in-situ measurements at mountain-top research station may well repre-
 473 sent the real properties of a cloud in contact with the surface and ~~now, when not.~~
- 474 • Further and more extensive field campaigns are necessary to better understand the
 475 mechanisms, which are responsible for the enhanced ICNC observed close to the
 476 surface at mountain-top research stations and their impact on cloud properties, e.g.
 477 extend lifetime and precipitation initiation.

*Setze doch den letzten
Punkt in Kapitel 4*

478 Acronyms

- 479 **ICNC** Ice Crystal Number Concentration
 480 **HOLIMO** HOLographic Imager for Microscopic Objects
 481 **SBO** Sonnblick Observatory

482 Acknowledgments

483 Sonnblick Observatory and team (Elke Ludewig, Hermann Scheer, Norbert Daxbacher,
 484 Lug Rasser, Hias Daxbacher)

485 Thanks to Hannes, Olga, Fabiola, Monika, for their help

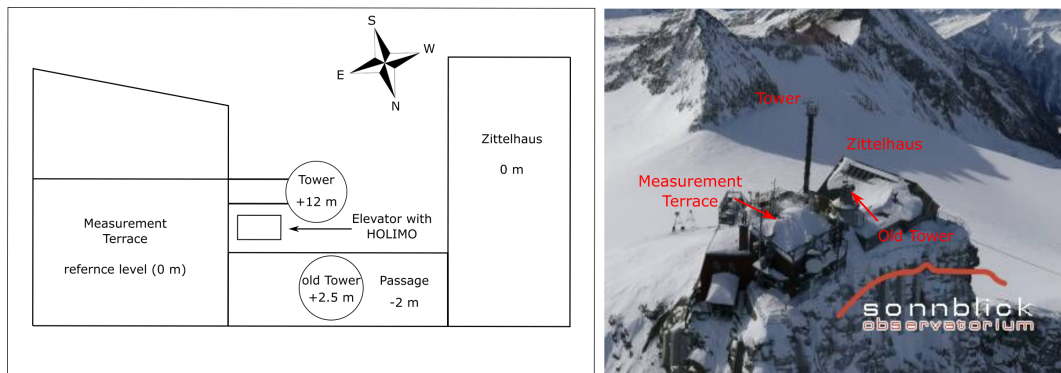
486 Thanks to Rob for many discussions

487 References

- 488 Baumgardner, D., J. Brenguier, A. Bucholtz, H. Coe, P. DeMott, T. Garrett, J. Gayet,
 489 M. Hermann, A. Heymsfield, A. Korolev, M. Krämer, A. Petzold, W. Strapp,
 490 P. Pilewskie, J. Taylor, C. Twohy, M. Wendisch, W. Bachalo, and P. Chuang (2011),
 491 Airborne instruments to measure atmospheric aerosol particles, clouds and radiation:
 492 A cook's tour of mature and emerging technology, *Atmos. Res.*, 102(1–2), 10 – 29,
 493 doi:10.1016/j.atmosres.2011.06.021.
- 494 Beck, A., J. Henneberger, S. Schöpfer, J. Fugal, and U. Lohmann (2017), Hologondel, *At-*
 495 *mos. Meas. Tech.*
- 496 Bromwich, D. H. (1988), Snowfall in high southern latitudes, *Reviews of Geophysics*,
 497 26(1), 149–168, doi:10.1029/RG026i001p00149.
- 498 Budd, W. F. (2013), *The Drifting of Nonuniform Snow Particles*, pp. 59–70, American
 499 Geophysical Union, doi:10.1029/AR009p0059.
- 500 Déry, S. J., and M. K. Yau (1999), A climatology of adverse winter-type weather
 501 events, *Journal of Geophysical Research: Atmospheres*, 104(D14), 16,657–16,672, doi:
 502 10.1029/1999JD900158.

- Farrington, R. J., P. J. Connolly, G. Lloyd, K. N. Bower, M. J. Flynn, M. W. Gallagher, P. R. Field, C. Dearden, and T. W. Choularton (2015), Comparing model and measured ice crystal concentrations in orographic clouds during the inupiaq campaign, *Atmos. Chem. and Phys.*, 15(18), 25,647–25,694, doi:10.5194/acpd-15-25647-2015.
- Field, P. R., R. P. Lawson, P. R. A. Brown, G. Lloyd, C. Westbrook, D. Moisseev, A. Miltenberger, A. Nenes, A. Blyth, T. Choularton, P. Connolly, J. Buehl, J. Crosier, Z. Cui, C. Dearden, P. DeMott, A. Flossmann, A. Heymsfield, Y. Huang, H. Kalesse, Z. A. Kanji, A. Korolev, A. Kirchgaessner, S. Lasher-Trapp, T. Leisner, G. McFarquhar, V. Phillips, J. Stith, and S. Sullivan (2017), Secondary ice production: Current state of the science and recommendations for the future, *Meteorological Monographs*, 58, 7.1–7.20, doi:10.1175/AMSMONOGRAPH-D-16-0014.1.
- Fugal, J. P. (2017), Holosuite, in preparation.
- Geerts, B., B. Pokharel, and D. a. R. Kristovich (2015), Blowing Snow as a Natural Glaciogenic Cloud Seeding Mechanism, *Mon. Weather Rev.*, 143(12), 5017–5033, doi:10.1175/MWR-D-15-0241.1.
- Gultepe, I., G. Isaac, and S. Cober (2001), Ice crystal number concentration versus temperature for climate studies, *International Journal of Climatology*, 21(10), 1281–1302, doi:10.1002/joc.642.
- Hallet, J., and S. Mossop (1974), Production of secondary ice particles during the riming process, *Nature*, 249, 26–28, doi:10.1038/249026a0.
- Hammer, E., N. Bukowiecki, M. Gysel, Z. Jurányi, C. R. Hoyle, R. Vogt, U. Baltensperger, and E. Weingartner (2014), Investigation of the effective peak supersaturation for liquid-phase clouds at the high-alpine site jungfraujoch, switzerland (3580 m a.s.l.), *Atmospheric Chemistry and Physics*, 14(2), 1123–1139, doi:10.5194/acp-14-1123-2014.
- Lachlan-Cope, T., R. Ladkin, J. Turner, and P. Davison (2001), Observations of cloud and precipitation particles on the avery plateau, antarctic peninsula, *Antarctic Science*, 13(3), 339–348, doi:10.1017/S0954102001000475.
- Li, L., and J. W. Pomeroy (1997), Estimates of threshold wind speeds for snow transport using meteorological data, *Journal of Applied Meteorology*, 36(3), 205–213, doi:10.1175/1520-0450(1997)036<0205:EOTWSF>2.0.CO;2.
- Lloyd, G., T. W. Choularton, K. N. Bower, M. W. Gallagher, P. J. Connolly, M. Flynn, R. Farrington, J. Crosier, O. Schlenczek, J. Fugal, and J. Henneberger (2015), The origins of ice crystals measured in mixed-phase clouds at the high-alpine site jungfraujoch, *Atmos. Chem. Phys.*, 15(22), 12,953–12,969, doi:10.5194/acp-15-12953-2015.
- Lohmann, U. (2002), Possible aerosol effects on ice clouds via contact nucleation, *Journal of the Atmospheric Sciences*, 59(3), 647–656, doi:10.1175/1520-0469(2001)059<0647:PAEOIC>2.0.CO;2.
- Mahesh, A., R. Eager, J. R. Campbell, and J. D. Spinhirne (2003), Observations of blowing snow at the south pole, *Journal of Geophysical Research: Atmospheres*, 108(D22), n/a–n/a, doi:10.1029/2002JD003327, 4707.
- Nishimura, K., and M. Nemoto (2005), Blowing snow at mizuho station, antarctica, *Philosophical Transactions of the Royal Society of London A: Mathematical, Physical and Engineering Sciences*, 363(1832), 1647–1662, doi:10.1098/rsta.2005.1599.
- Palm, S. P., Y. Yang, J. D. Spinhirne, and A. Marshak (2011), Satellite remote sensing of blowing snow properties over antarctica, *Journal of Geophysical Research: Atmospheres*, 116(D16), n/a–n/a, doi:10.1029/2011JD015828, d16123.
- Rangno, A. L., and P. V. Hobbs (2001), Ice particles in stratiform clouds in the arctic and possible mechanisms for the production of high ice concentrations, *Journal of Geophysical Research: Atmospheres*, 106(D14), 15,065–15,075, doi:10.1029/2000JD900286.
- Rogers, D. C., and G. Vali (1987), Ice crystal production by mountain surfaces, *J. Clim. Appl. Meteorol.*, 26(9), 1152–1168, doi:10.1175/1520-0450(1987)026<1152:ICPBMS>2.0.CO;2.

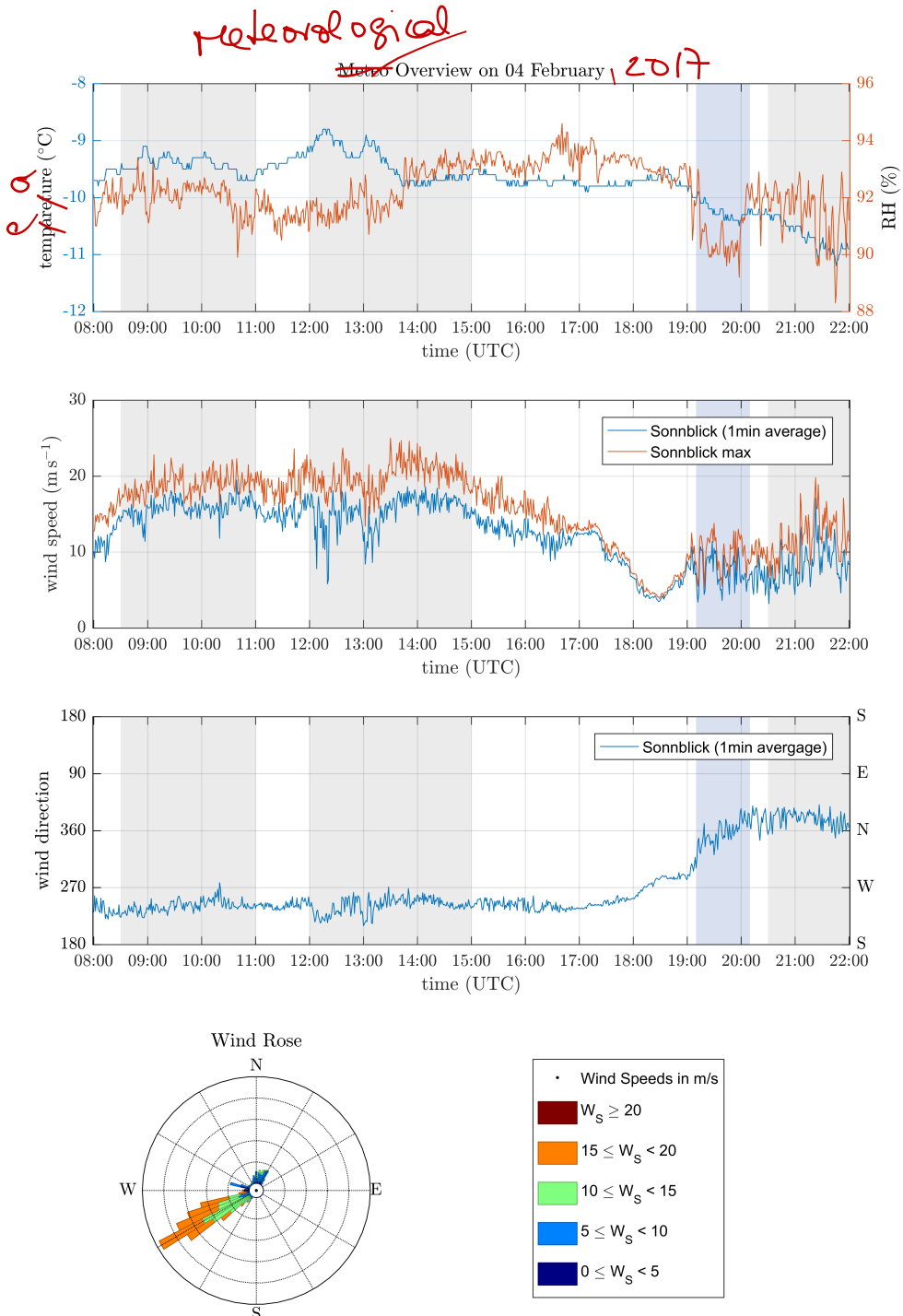
- 556 Rotunno, R., and R. A. Houze (2007), Lessons on orographic precipitation from the
557 mesoscale alpine programme, *Quarterly Journal of the Royal Meteorological Society*,
558 133(625), 811–830, doi:10.1002/qj.67.
- 559 Schlenzeck, O., and J. Fugal (2017), Microphysical properties of ice crystal precipitation
560 and surface-generated ice crystals in a high alpine environment in switzerland, *esult*, 56,
561 433–453, doi:10.1175/JAMC-D-16-0060.1.
- 562 Schmidt, R. A. (1982), Vertical profiles of wind speed, snow concentration, and
563 humidity in blowing snow, *Boundary-Layer Meteorology*, 23(2), 223–246, doi:
564 10.1007/BF00123299.
- 565 Vali, G., D. Leon, and J. R. Snider (2012), Ground-layer snow clouds, *Quarterly Journal*
566 *of the Royal Meteorological Society*, 138(667), 1507–1525, doi:10.1002/qj.1882.
- 567 Vionnet, V., G. GuyomarcâŽh, F. N. Bouvet, E. Martin, Y. Durand, H. Bellot, C. Bel,
568 and P. PugliaÃlise (2013), Occurrence of blowing snow events at an alpine site over a
569 10-year period: Observations and modelling, *Advances in Water Resources*, 55, 53 – 63,
570 doi:<http://doi.org/10.1016/j.advwatres.2012.05.004>, snowâŠAtmosphere Interactions
571 and Hydrological Consequences.
- 572 Yang, J., and M. K. Yau (2008), A new triple-moment blowing snow model, *Boundary-*
573 *Layer Meteorology*, 126(1), 137–155, doi:10.1007/s10546-007-9215-49.



574 **Figure 1.** Sketch of the experimental setup and the surrounding structures (left) with their heights relative
575 to the bottom of the measurement terrace. Aerial image of the Sonnblick Observatory (right).

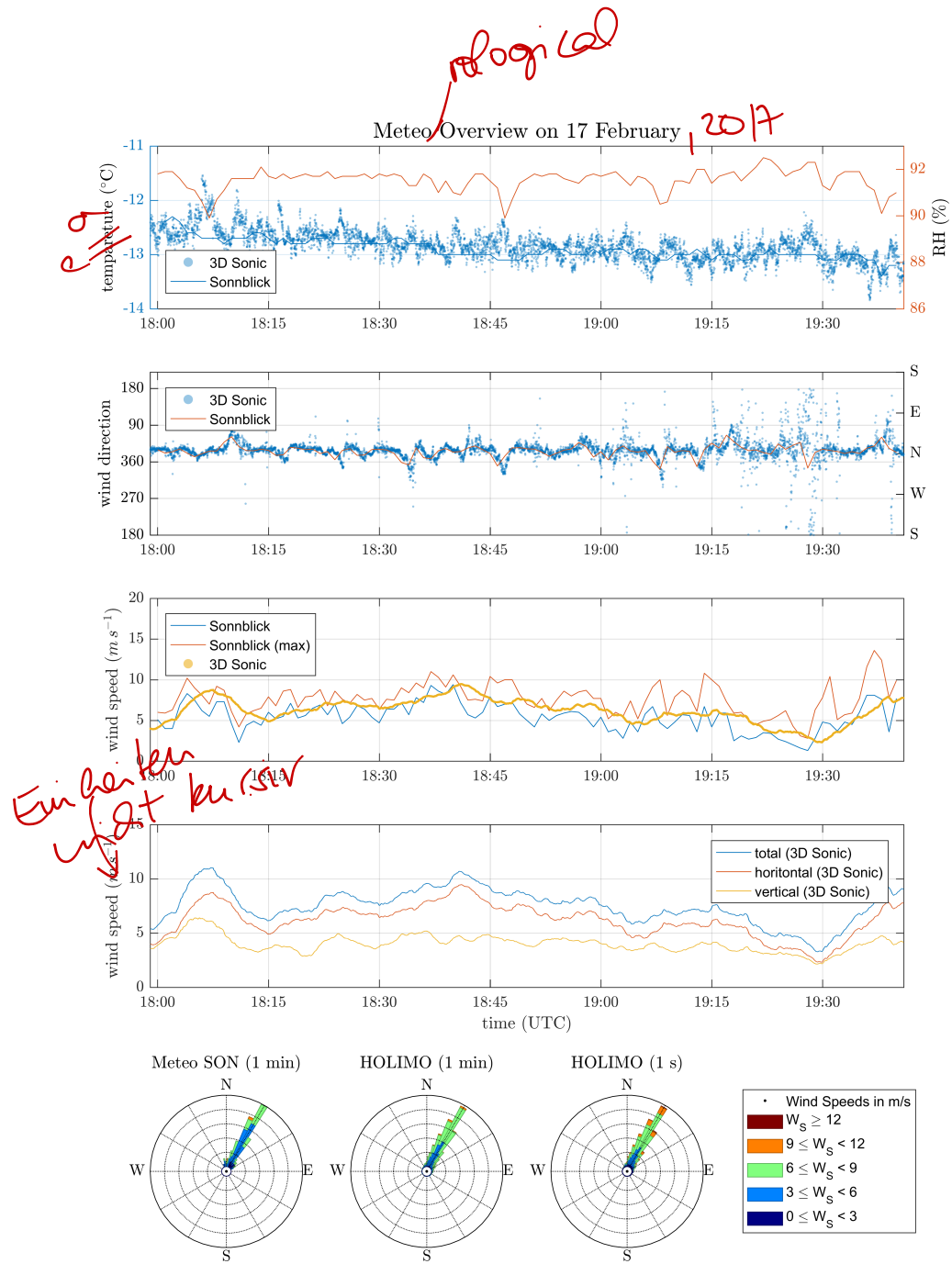


576 **Figure 2.** Set up of the elevator with the holographic imager HOLIMO mounted to the meteorological
577 tower at the SBO. The red lines and numbers indicate the five different heights where the elevator was posi-
578 tioned repeatedly to obtain vertical profiles of the ICNC. The reference height of 0.0 m is the bottom of the
579 measurement platform (green line).



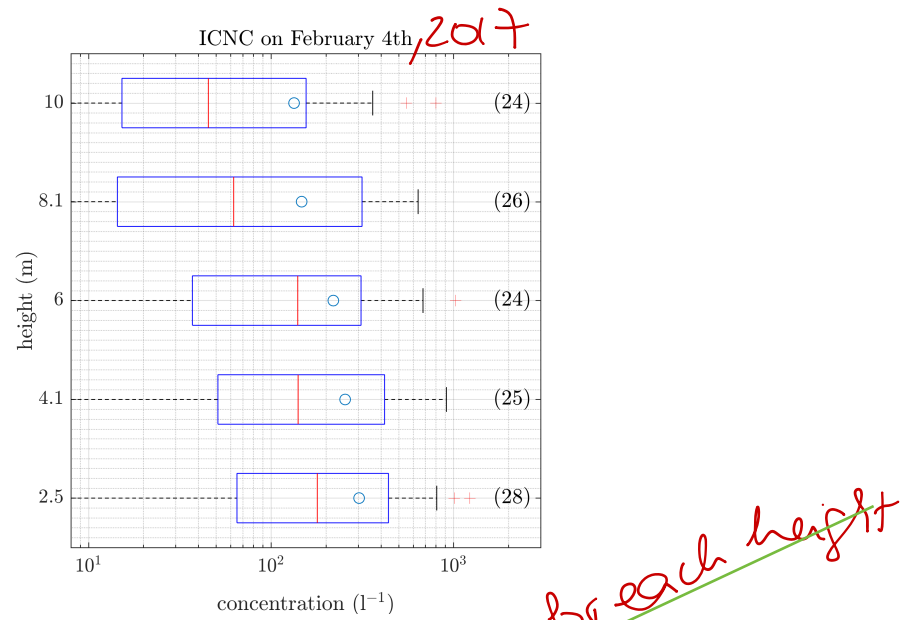
580 **Figure 3.** Overview of the meteorological conditions on 4 February obtained from the SBO measurements.
 581 All measurements are 1 min averages except for the maximum wind speed, which corresponds to the maxi-
 582 mum wind speed observed during a corresponding 1 min average. The shaded areas represent intervals with
 583 ice crystal measurements with the SBO in cloud (gray), respectively not in cloud (blue).

need to add description of wind rose

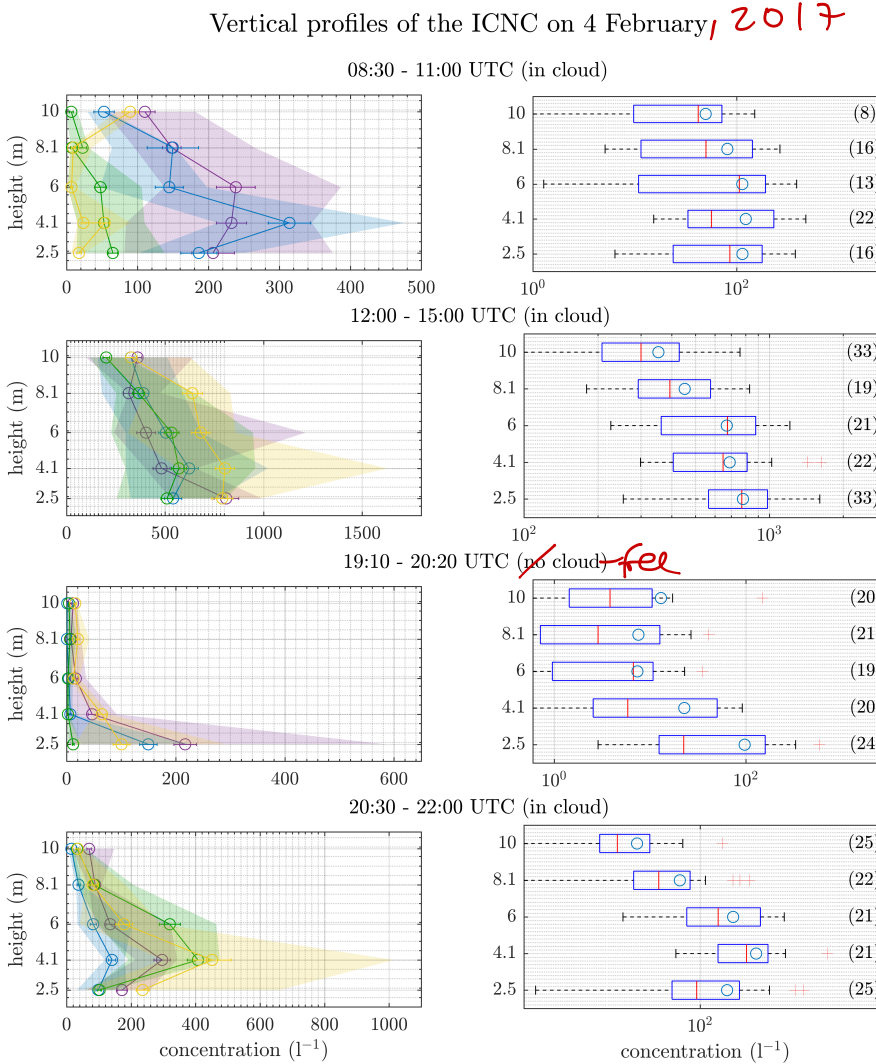


584 **Figure 4.** Overview on the meteorological conditions on 17 February 2017 for the time interval when measure-
 585 ments exist (see Fig. 8). On this day temperature and wind measurements are available from the SBO and the
 586 3D Sonic Anemometer. Shown are the temperature and relative humidity (top), wind direction (second from
 587 top), a comparison of the horizontal wind speed (middle) and detailed wind speed measurements from the 3D
 588 Sonic Anemometer (second from bottom). A windrose plot is shown in the bottom panel.

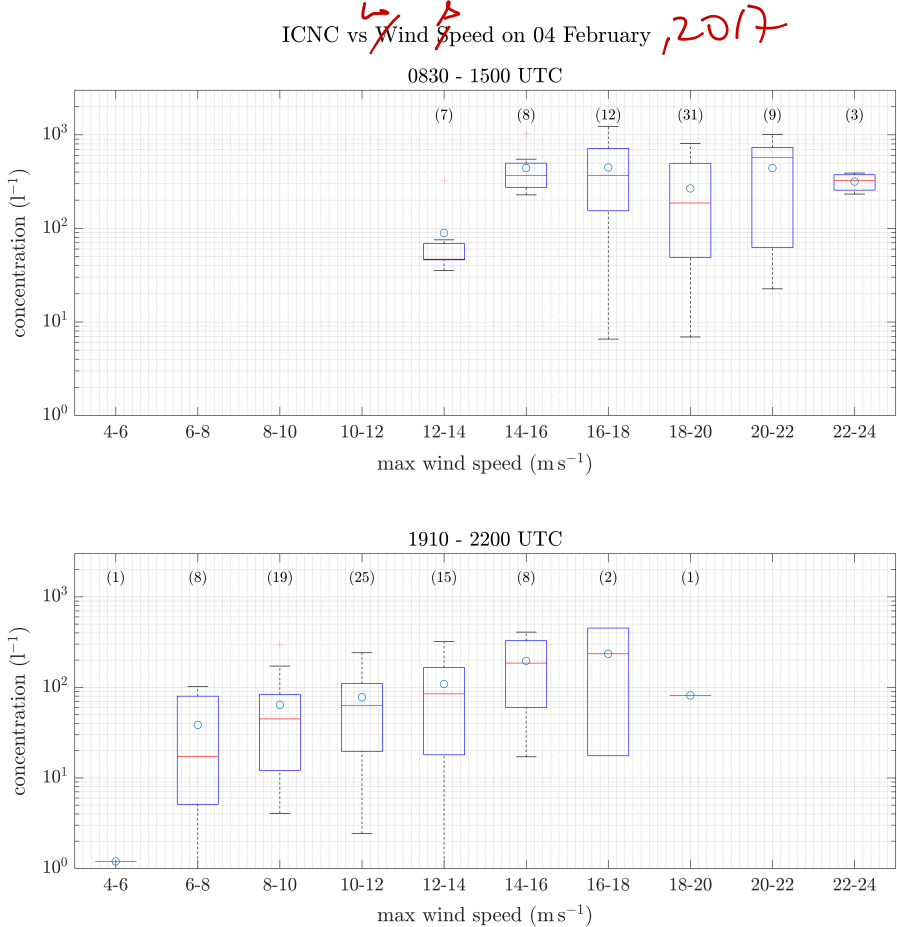
also add to Fig. 3



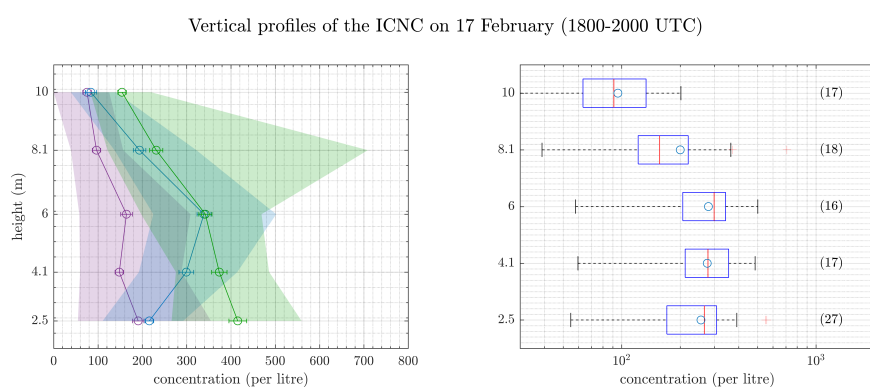
589 **Figure 5.** ICNC as a function of the height of the elevator at the meteorological tower of the SBO. This plot
 590 is a summary of the 24 profiles obtained on 4 February. The data was averaged over the entire time period
 591 of single measurements at the different height. The number in brackets is the number of concentration
 592 measurements per height. For each box, the central line marks the median value of the measurement and the
 593 left and right edges of the box represent 25th and the 75th percentiles respectively. The whiskers extend to the
 594 minimum and maximum of the data; outliers are marked as red pluses. The mean value of the measurements
 595 is indicated as a blue circle.
 one



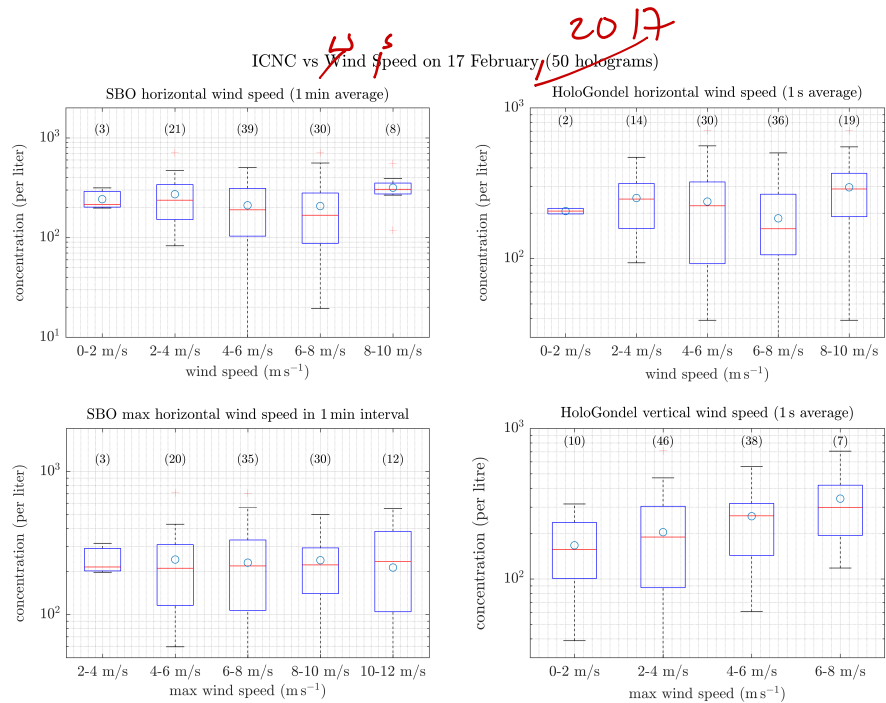
596 **Figure 6.** ICNCs as a function of height of the elevator for four different time intervals during 4 February,
597 representing different conditions (Fig. 3). On the individual profiles (left), the circles indicate the mean and
598 the error bars the standard error of the mean. The shaded area extends from the minimum to the maximum of
599 the measured ICNC. The box plots (right) show a summary of all profiles in the respective time interval as in
600 Figure 5.



601 **Figure 7.** As Figure 5, only ICNC as a function of horizontal wind speed for the time periods between
602 0830 and 1500 UTC when the wind direction was West-Southwest (top) and between 1910 and 2200 UTC
603 when the wind direction was North (bottom). The ICNCs from HOLIMO are one minute averages and the
604 wind speeds from the SBO is the maximum in the respective one minute interval.
but for the from the are from the

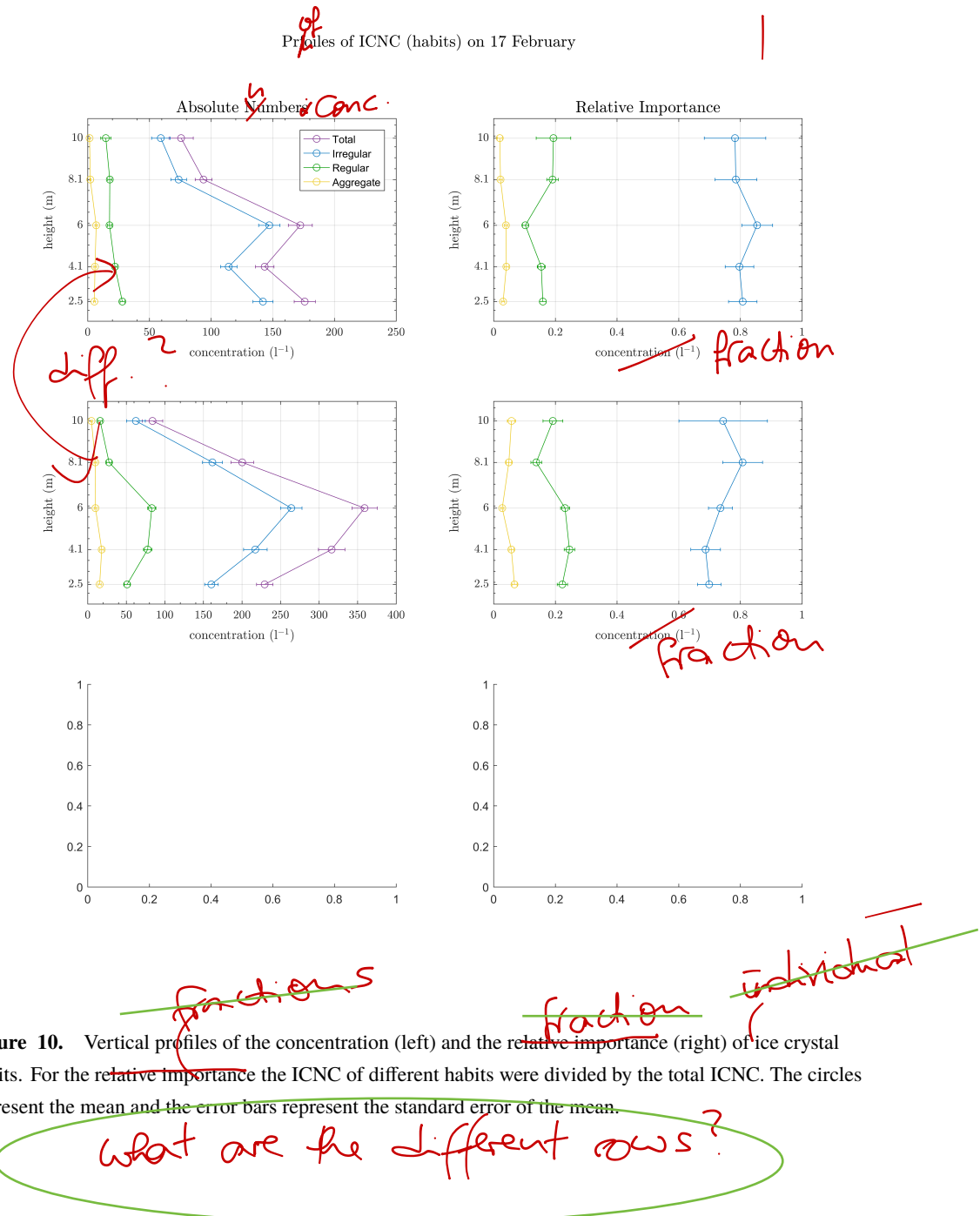


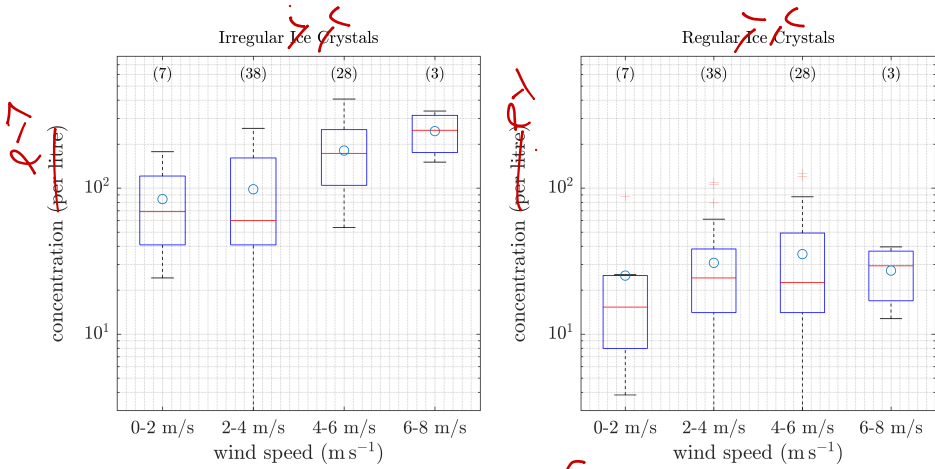
605 **Figure 8.** ICNC as a function of height observed on 17 February presented in Figure 6.
As figure 6, but for



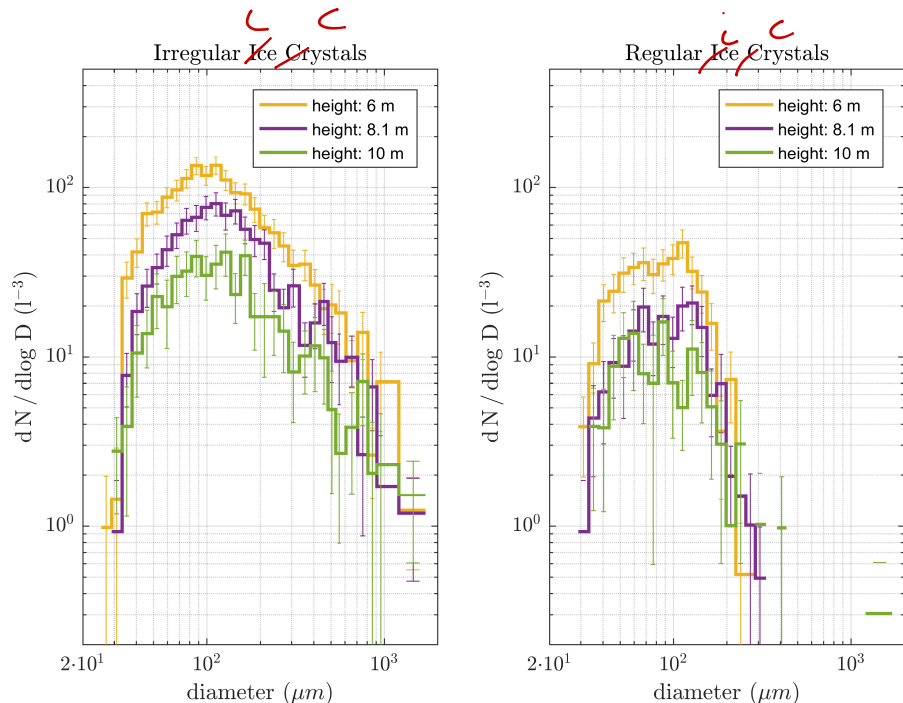
606 **Figure 9.** As Figure 7 only for 17 February and four different wind speed measurements: a) one minute
607 averages of the horizontal wind speed from the SBO, b) maximum wind speed of the corresponding time
608 interval in a), c) secondly averages of the horizontal wind speed and d) secondly average of the vertical wind
609 speed both from the 3D Sonic Anemometer.

*Welcher ist c), b)
tatsächlich b) & c)*

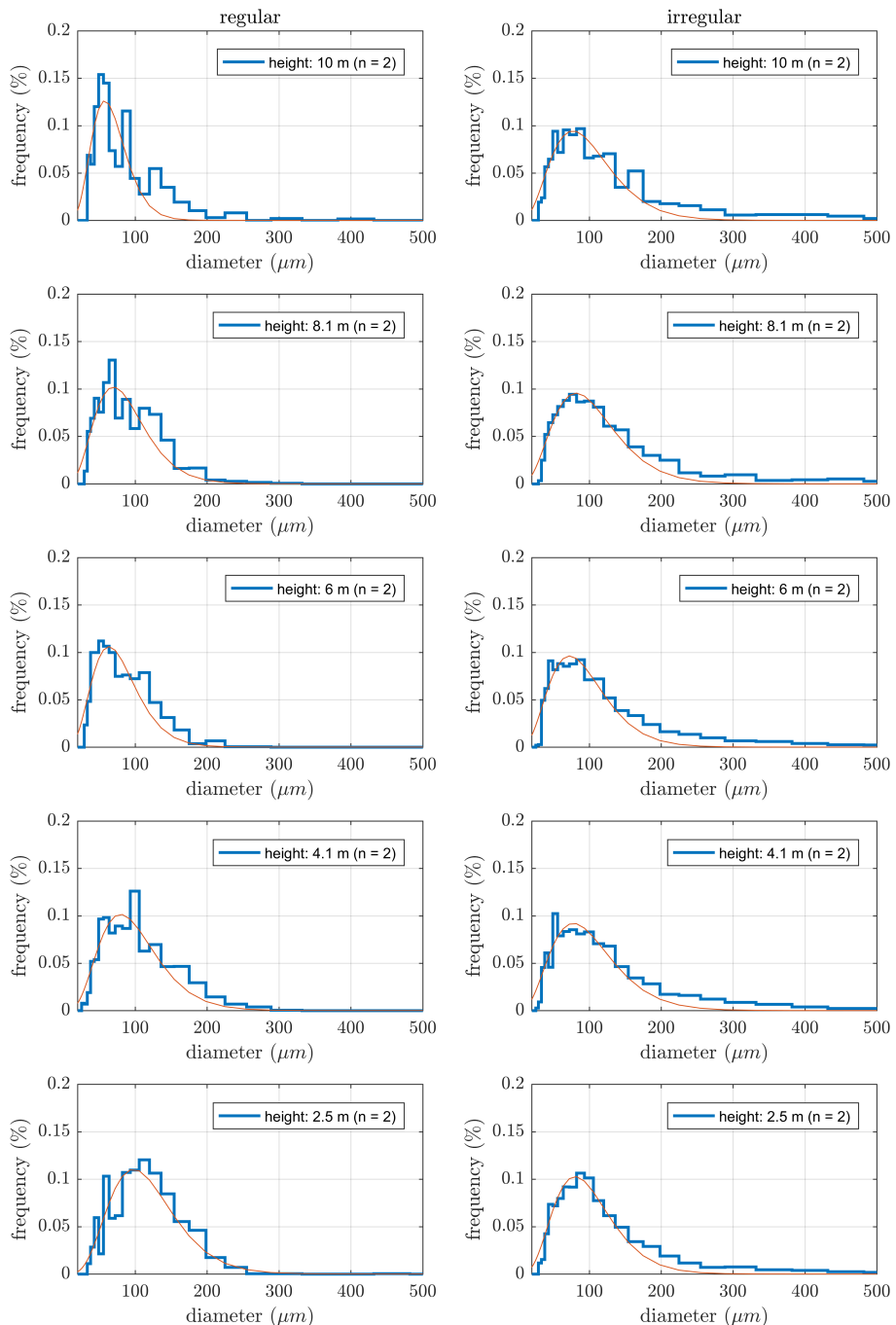




613 **Figure 11.** As Figure 7 only for 17 February and the ICNC of different ice crystal habits as a function of the
 614 vertical wind speed. Aggregates are not shown because of their very low concentration. *2017, for*

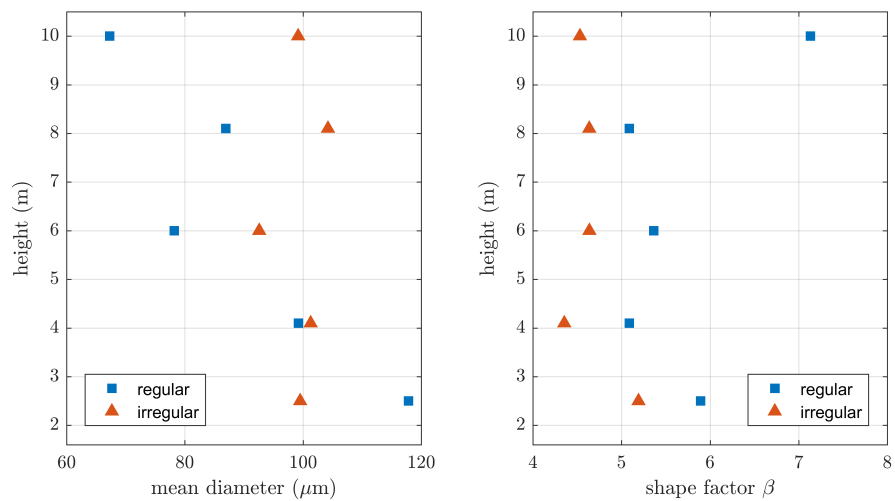


615 **Figure 12.** Size distribution of the irregular (left) and regular (right) ice crystals observed on 17 February
 616 as a function of height. The errorbars represent the standard error of the mean. Aggregates are not shown
 617 because of their very low concentration. *2017*



618 **Figure 13.** Probability distribution of the particle diameter for regular (left) and irregular (right) ice crystals
619 measured on 17 February. The red line indicates the result of the fit of the two parameter gamma pdf from
620 equation (1). Aggregates are not shown because of their very low concentration.
621

prob. density fct



621 **Figure 14.** Profiles of the mean diameter (left) and the shape parameter (right)
622 gamma γ_{PDF} (Eq. (1)) plotted as a function of height.

Fassschreiben